Mechanoenzymatic Characterization of Human Myosin Vb†

Shinya Watanabe,‡ Katsuhide Mabuchi,§ Reiko Ikebe,‡ and Mitsuo Ikebe*,‡

Department of Physiology, University of Massachusetts Medical School, 55 Lake Avenue North, Worcester, Massachusetts 01655-0127, and Boston Biomedical Research Institute, 64 Grove Street, Watertown, Massachusetts 02472-2829

Received August 23, 2005; Revised Manuscript Received December 30, 2005

ABSTRACT: There are three isoforms of class V myosin in mammals. While myosin Va has been studied well, little is known about the function of other myosin V isoforms (Vb and Vc) at a molecular level. Here we report the mechanoenzymatic function of human myosin Vb (HuM5B) for the first time. Electron microscopic observation showed that HuM5B has a double-headed structure with a long neck like myosin Va. V_{max} and K_{actin} of the actin-activated ATPase activity of HuM5B were 9.7 ± 0.4 s^{-1} and 8.5 ± 0.1 μM, respectively. K_{actin} and K_{ATP} of the actin-activated ATPase activity were significantly higher than those of myosin Va. ADP markedly inhibited the ATPase activity. The rate of release of ADP from acto-HuM5B was 12.2 ± 0.5 s^{-1}, which was comparable to the V_{max} of the actin-activated ATPase activity. These results suggest that ADP release is the rate-limiting step for the actin-activated ATPase cycle; thus, HuM5B is a high duty ratio myosin. Consistently, the actin gliding velocity (0.22 ± 0.03 μm/s) remained constant at a low motor density. The actin filament landing assay revealed that a single HuM5B molecule is sufficient to move the actin filament continuously, indicating that HuM5b is a processive motor.

Myosin is a mechanoenzymatic protein that interacts with actin and converts the chemical energy from ATP hydrolysis to the mechanical work. In addition to well-characterized conventional, filament-forming, two-headed myosin II of muscle and non-muscle cells, a number of myosin-like proteins have been discovered, and it is known that myosin constitutes a diverse superfamily divided into at least 18 classes (*1*−*7*). Class V myosins are one of the most ancient myosins of the superfamily, and their genes have been identified in species from yeast, *Caenorhabditis elegans*, and *Drosophila* to humans (*7*). *Dictyostelium* MyoJ and plant class XI and VIII myosins are structurally and functionally related to class V myosins. Yeast contains two class V myosins, while *C. elegans* and *Drosophila* contain a single class V myosin. In mammals, there are three distinct subclasses of myosin V. Mammalian class V myosin was first discovered from *dilute* mice that have a lighter color coat due to the lack of proper pigment transport (*8*). This myosin V is now classified as myosin Va, and most of the biochemical and cell biological works for class V myosin have been done with this myosin V isoform (see ref *9* for a review). There are two additional myosin V isoforms reported, i.e., myosin Vb and myosin Vc (*10*, *11*), yet their properties at a molecular level have not been studied.

The structure of myosin Va was visualized by electron microscopy, and it was shown that myosin Va is the two-headed structure with the long neck connecting the head and the coiled-coil domain. On the basis of the amino acid sequence homology with myosin Va (*10*, *11*), it is thought that, overall, the structure of myosin Vb and myosin Vc resembles that of myosin Va. The heavy chain of myosin Vb has a molecular mass of 214 kDa and composed of the N-terminal conserved motor domain, the neck domain containing six IQ motifs that are thought to be the light chain binding sites, and the tail domain consisting of a proximal segment of the coiled-coil domain followed by a PEST domain, a second coiled-coil domain, and the globular tail. Because of the presence of the coiled-coil domain, it is assumed that myosin Vb exists as a dimer, i.e., two-headed structure.

The motor function of class V myosin has been studied best for myosin Va. A most intriguing finding for myosin Va is that this myosin has a high duty ratio (*12*) and actually moves along actin filaments for many steps without dissociating from actin and is, thus, processive (*13*, *14*). This processive behavior is consistent with the function of myosin Va in the cell as a cargo transporter (*9*). A finding critical to understand the mechanism of processive movement of myosin Va is the extremely large step size of myosin Va (*13*, *15*, *16*). Because myosin Va has an extremely long neck domain, it was proposed that myosin Va moves with a hand-over-hand mechanism in which myosin heads span a helical repeat of the actin filament with its long neck and walk straight along it with one head attached and the other head dissociated (*17*−*19*). However, the recent reports have suggested that the long neck may not be essential for the multiple successive large steps of myosin V (*15*, *20*), and the mechanism of the processive movement of myosin V is controversial.

† This work was supported by National Institutes of Health Grants AR 048526, AR 048898, and DC 006103 (to M.I.).

* To whom correspondence should be addressed: Department of Physiology, University of Massachusetts Medical School, 55 Lake Ave. N., Worcester, MA 01655-0127. Phone: (508) 856-1954. Fax: (508) 856-4600. E-mail: Mitsuo.Ikebe@umassmed.edu.

‡ University of Massachusetts Medical School.

§ Boston Biomedical Research Institute.

10.1021/bi051682b CCC: $33.50 © 2006 American Chemical Society
Published on Web 02/03/2006

Myosin Va is expressed chiefly in brain and melanocytes, where myosin Va plays a crucial role in types of membrane trafficking such as melanosome transport (*21*, *22*) and smooth endoplasmic reticulum transport (*23*). On the other hand, myosin Vb is widely expressed in a variety of tissues, including lung, kidney, intestine, testes, liver, and heart (*10*). While nothing is known about the motor function of myosin Vb at a molecular level, most of the studies for myosin Vb have centered on the identity of the target molecules. Several recent reports have suggested that myosin Vb is involved in plasma membrane recycling systems that play fundamental roles in the maintenance of normal membrane composition. Myosin Vb associates with members of the small GTPase Rab11 family which are the markers for plasma membrane recycling systems (*24*). The overexpression of the myosin Vb tail retarded the transferrin recycling and caused concentration of transferrin receptors in pericentrosomal vesicles in HeLa cells (*24*). Myosin Vb also regulates the recycling of chemokine receptor CXCR2 (25) and the M4 muscarinic acetylcholine receptor (*26*). Moreover, the inhibition of myosin Vb activity attenuates the accumulation of transferrin in the cytoplasm and increases the level of the plasma membrane transferrin receptor (*27*). These findings suggest that myosin Vb functions as a cargo transporter in cells and carries cargo molecules different from those of myosin Va. However, nothing is known about the motor function and characteristic of myosin Vb that is crucial to understanding the physiological function of myosin Vb. Since a recent report of *Drosophila* myosin V indicated that it is a nonprocessive myosin, although it is classified as a class V myosin (*28*), a critical question is whether myosin Vb is a processive myosin suitable for the transportation of cargo. In this study, we show that myosin Vb is a processive motor similar to myosin Va. Here we report for the first time the motor function and characteristic of myosin Vb at a molecular level.

EXPERIMENTAL PROCEDURES

Materials. Restriction enzymes and modifying enzymes were purchased from New England Biolabs. Anti-FLAG M2 affinity gel, FLAG peptide, phosphoenolpyruvate, and pyruvate kinase were purchased from Sigma. Actin was prepared from rabbit skeletal muscle according to the method of Spudich and Watt (*29*).

Generation of the Expression Vectors for Myosin Vb Constructs. Human myosin Vb cDNA clones were obtained from human kidney total RNA by RT-PCR using Pfu-ultra DNA polymerase (Stratagene) with primers having a BamHI site for M5B1 and SalI site for M5B2. The two cDNAs (M5B1 and M5B2) containing nucleotides −3 to 2868 and 2747−5608, respectively, were cloned into the pCR2.1TOPO vector (Invitrogen). A FLAG tag sequence and a ClaI site were introduced into the pFastHTc baculovirus transfer vector (Invitrogen) at the 5′ side of the polylinker region and within the polylinker region, respectively. M5B1 was digested with BamHI and ClaI. The fragment was subcloned into the modified pFastbac HTc. M5B2 was digested with ClaI and SalI and introduced into the vector having M5B1. Stop codons were introduced into M5B2 at nucleotide 2916 for the S1[1] construct and at nucleotide 3339 for the HMM construct. Finally, the full sequences of M5BS1 and M5BHMM were confirmed.

Expression and Purification of Myosin Vb. To express the recombinant myosin Vb protein, Sf9 cells ($\sim 1 \times 10^9$ cells) were co-infected with two viruses expressing the myosin Vb heavy chain and calmodulin. The infected cells were cultured for 3 days at 28 °C. Cells were harvested and washed with TBS and 5 mM EGTA. Cells were then lysed with sonication in 40 mL of lysis buffer [30 mM Tris-HCl (pH 7.5), 150 mM NaCl, 1 mM EGTA, 2 mM $MgCl_2$, 1 mM ATP, 0.5 mM dithiothreitol, 1 mM phenylmethanesulfonyl fluoride, 10 μg/mL leupeptin, 2 μg/mL pepstatin A, 1 μg/mL trypsin inhibitor, 0.1 mM TPCK, and 0.1 mM TLCK]. After centrifugation at 100000*g* for 30 min, the supernatant was incubated with 1.0 mL of anti-FLAG M2 affinity resin in a 50 mL conical tube on a rotating wheel for 1 h at 4 °C. The resin suspension was then loaded onto a column (1 cm × 10 cm) and washed with 40 mL of buffer A [30 mM Tris-HCl (pH 7.5), 150 mM KCl, 1 mM EGTA, 2 μg/mL leupeptin, and 0.5 mM dithiothreitol]. Myosin Vb was eluted with buffer A containing 0.1 mg/mL FLAG peptide and concentrated with a VIVASPIN concentrator (Vivascience). The collected myosin Vb was dialyzed against buffer B [50 mM KCl, 20 mM MOPS-KOH (pH 7.0), 3 mM $MgCl_2$, 1 mM EGTA, and 1 mM dithiothreitol]. The purified myosin Vb was stored on ice and used within 2 days.

Gel Electrophoresis. SDS−polyacrylamide gel electrophoresis was carried out on a 7.5 to 20% polyacrylamide gradient slab gel using the discontinuous buffer system of Laemmli (*30*). Molecular mass markers that were used were smooth muscle myosin heavy chain (204 kDa), β-galactosidase (116 kDa), phosphorylase *b* (97.4 kDa), bovine serum albumin (66 kDa), ovalbumin (45 kDa), carbonic anhydrase (29 kDa), myosin regulatory light chain (20 kDa), and α-lactalbumin (14.2 kDa). The gel was stained with Coomassie Brilliant Blue. The amount of myosin Vb heavy chain was determined by densitometry analysis of SDS−PAGE using the smooth muscle myosin heavy chain as a standard.

Electron Microscopy. Myosin Vb proteins diluted to ~4 nM were absorbed onto a freshly cleaved mica surface for 30 s. Unbound proteins were rinsed away, and then the specimen was stabilized by brief exposure to uranyl acetate as described previously (*31*). The specimen was visualized by the rotary shadowing technique according to the method of Mabuchi (*32*) with a Philips 300 electron microscope at 60 kV.

ATPase Assay. The steady-state ATPase activity was measured at 25 °C in the presence of an ATP regeneration system containing 40 units/mL pyruvate kinase and 4 mM phosphoenolpyruvate. The reaction was carried out in buffer B. The amount of liberated pyruvate was determined as described previously (*33*). The steady-state ATPase assay in the absence of an ATP regeneration system was initiated by adding [γ-^{32}P]ATP to the reaction mixture. The amount of liberated ^{32}P was measured as described previously (*34*).

In Vitro Motility Assay. The actin gliding velocity was measured by the in vitro actin gliding assay as described

[1] Abbreviations: S1, subfragment 1; HMM, heavy meromyosin; TBS, Tris-buffered saline; MOPS, 4-morpholinepropanesulfonic acid; TPCK, L-1-tosylamido-2-phenylethyl chloromethyl ketone; TLCK, 1-chloro-3-tosylamido-7-amino-2-heptanone.

previously (*35*). A glass surface was first coated with nitrocellulose and blocked with 0.01 mg/mL BSA, and then M5BHMM was applied to the flow cells. The movement of the rhodamine-labeled actin filaments was observed in buffer C [25 mM KCl, 25 mM imidazole (pH 7.5), 5 mM $MgCl_2$, 1 mM EGTA, 1 mM dithiothreitol, 36 μg/mL catalase, 4.5 mg/mL glucose, 216 μg/mL glucose oxidase, 0.5% methylcellulose, and 4 mM MgATP] at 25 °C. The dependence of the actin gliding velocity on ATP was examined in buffer B containing various concentrations of ATP, 36 μg/mL catalase, 4.5 mg/mL glucose, 216 μg/mL glucose oxidase, and the ATP regeneration system at 25 °C. Dual-labeled F-actin was prepared as described previously (*36*). The actin gliding velocity was calculated from the movement distance and the elapsed time in successive snapshots. A Student's *t* test was used for statistical comparison of mean values. A *p* value of <0.01 was considered to be significant. The landing assay was performed in buffer C containing 1 nM actin without methylcellulose. To quantify landing rates, we scored a filament as "landed" when the filament landed and moved for more than 0.5 μm over the course of 3 s. The theoretical fit in the landing assay was performed on the basis of the equations described previously (*37*, *38*). The surface density of myosin molecules was calculated assuming that every myosin molecule entered into the flow cell and half of them were adsorbed onto the surface of the flow cell, based on the densitometry analysis of SDS−PAGE showing approximately half of the loaded proteins was adsorbed by the flow cells.

Pre-Steady-State Kinetic Measurements. Kinetic measurements were performed in buffer B at 25 °C using a stopped-flow spectrophotometer (Kin-Tek Corp.) with a 75 W xenon lamp. Mant nucleotide was excited at 280 or 365 nm, and emission was collected through a 400 nm long-pass filter. Dissociation of acto-myosin Vb and acto-myosin Vb-ADP by ATP were assessed from the decrease in light scattering (*39*). All kinetic data shown are the average of three to five transients.

RESULTS

Expression and Purification of M5B Constructs. We produced two constructs of human myosin Vb. One is M5BS1 containing the motor domain and six IQ domains (Figure 1A). Because the coiled-coil domain is deleted, it is expected that M5BS1 is a single-headed myosin Vb construct. The other is M5BHMM that contains the entire first long coiled-coil domain of myosin Vb; therefore, it is anticipated that M5BHMM has a two-headed structure (Figure 1B). M5BS1 and M5BHMM constructs were coexpressed with calmodulin in Sf9 cells, and the expressed proteins were purified with anti-FLAG antibody-conjugated affinity chromatography. The isolated M5BS1 and M5BHMM were composed of a high-molecular mass peptide and a low-molecular mass peptide, respectively (Figure 2A). The high-molecular mass peptides had apparent molecular masses of 111 and 131 kDa that are consistent with the calculated molecular mass of M5BS1 (112 kDa) and M5BHMM (133 kDa) heavy chains, respectively. The low-molecular mass band was calmodulin since the mobility of this peptide was shifted in the presence of Ca^{2+}, which is characteristic of calmodulin due to the conformational change in Ca^{2+} (data not shown). The stoichiometries of calmodulin versus myosin

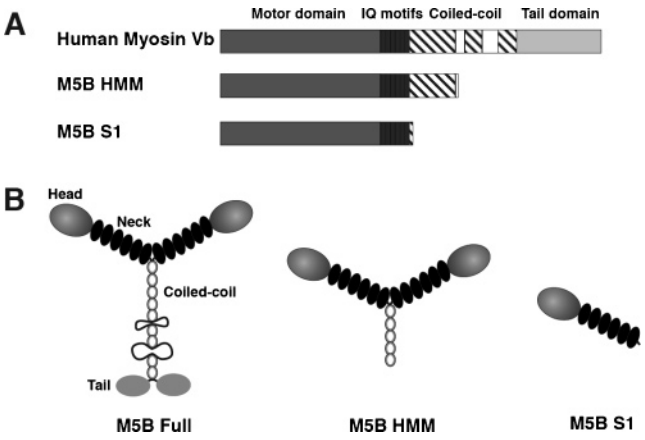

FIGURE 1: Schematic drawing of myosin Vb constructs. (A) Primary structures of myosin Vb constructs. A hexahistidine tag and FLAG tag were added at the N-terminal end of M5BS1 and M5BHMM. Stripes mark the predicted coiled-coil domains. (B) Schematic drawings of myosin Vb constructs. There are six IQ motifs at the neck that serve as calmodulin binding sites.

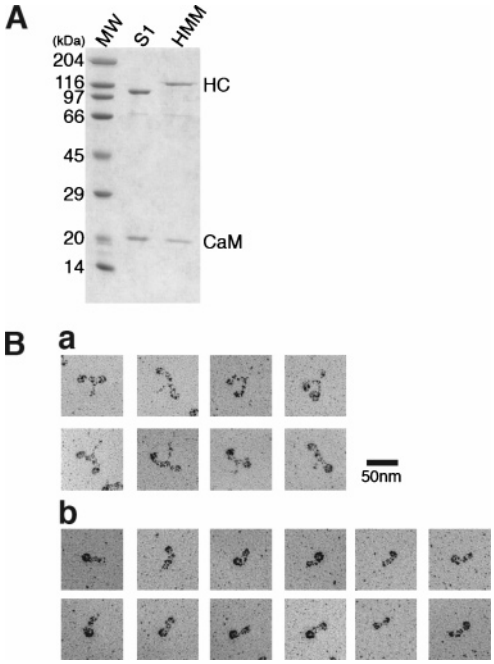

FIGURE 2: Purification and visualization of M5BS1 and M5BHMM. (A) SDS−PAGE of the purified constructs. M5S1 and M5HMM expressed in Sf9 cells were extracted and purified as described in Experimental Procedures, and the purified proteins were analyzed by SDS−PAGE. HC and CaM represent the heavy chain of myosin Vb constructs and calmodulin, respectively. (B) Electron micrographs of M5BHMM and M5BS1. The samples were diluted to ~4 nM with dilution buffer containing 0.1 M ammonia acetate (pH 7.2) and 30% glycerol: (a) M5BHMM and (b) M5BS1.

Vb heavy chain were determined by densitometry to be 6.1 ± 0.4 for M5BS1 and 5.9 ± 0.5 for M5BHMM. These values are consistent with the number of IQ motifs in myosin Vb. We also coexpressed non-muscle myosin essential light chain (LC17b) along with myosin Vb heavy chain and calmodulin, but we could not detect the essential light chain associated with the purified myosin Vb (data not shown). While chicken myosin Va purified from brain has two essential light chains (LC1sa and LC17b) in addition to calmodulin (*40*), mouse myosin Va purified from brain does not show the presence of any essential light chains (*41*). The result suggests that

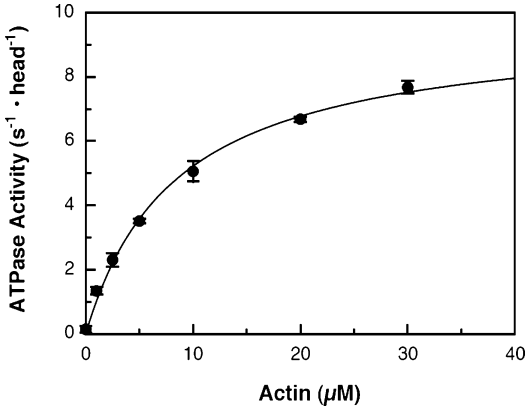

FIGURE 3: Actin concentration dependence of the ATPase activity of M5BS1. The actin-activated ATPase activity was measured in buffer containing 50 mM KCl, 20 mM MOPS (pH 7.0), 3 mM $MgCl_2$, 1 mM EGTA, 4 mM phosphoenolpyruvate, 40 units/mL pyruvate kinase, 20 nM M5BS1, and 2 mM MgATP at 25 °C. The solid line is the fit to the Michaelis−Menten equation with a V_{max} of 9.7 ± 0.4 s^{-1} and a K_{actin} of 8.5 ± 0.1 μM. Error bars are standard deviations of three independent experiments.

Table 1: Kinetic and Motility Parameters of Human Myosin Vb and Comparison with Mammalian Myosin Va and *Drosophila* Myosin V

	human myosin Vb	mammalian myosin Va[a]	*Drosophila* myosin V[b]
steady state			
v_0 (s^{-1})	0.09 ± 0.04	0.03	0.07 ± 0.013
V_{max} (s^{-1})	9.7 ± 0.4	15	12.9
K_{actin} (μM)	8.5 ± 0.1	1.4	19.2
K_{ATP} (μM)	28.1 ± 5.9	9.6 ± 0.8[c]	−
motility (μm/s)	0.22 ± 0.03	0.32 ± 0.08[d]	0.46 ± 0.10
ATP binding			
K_1k_{+2} (μM^{-1} s^{-1})	0.78 ± 0.02	1.6	1.31 ± 0.52
$K_1'k_2'$ (μM^{-1} s^{-1})	0.31 ± 0.02	0.9	0.36 ± 0.006
k_{-2} (s^{-1})	0.20 ± 0.12	−	−
k_{-2}' (s^{-1})	1.2 ± 0.1	−	−
ADP release			
k_5' (s^{-1})	12.2 ± 0.5	16	150

[a] From ref *12*. [b] From ref *28*. [c] From this study. [d] From ref *36*.

mammalian myosin Vb has calmodulin but not the essential light chains such as mammalian myosin Va. Figure 2B shows electron micrographs of M5BS1 and M5BHMM. As expected from the primary structure of the constructs, M5BHMM had a two-headed structure and M5BS1 was single-headed. As shown in Figure 2B, both M5BHMM and M5BS1 contained a long neck that is consistent with the presence of six IQ motifs.

Actin-Activated ATPase Activity of Myosin Vb. Figure 3 shows the actin-activated ATPase activity of M5BS1 as a function of actin concentration. The activity was significantly activated by actin, and the actin dependence exhibited a hyperbolic saturation curve versus the increasing actin concentration. The actual data points were fitted to the Michaelis−Menten equation to yield V_{max} and K_{actin} values of 9.7 ± 0.4 s^{-1} and 8.5 ± 0.1 μM, respectively. The V_{max} was approximately two-thirds of that of myosin Va (*12*, *42*) (Table 1). On the other hand, the K_{actin} was significantly higher than that of myosin Va (*12*, *41*, *43*) (Table 1); nevertheless, the value was much lower than those of conventional myosins (*44*−*50*). Although the light chain alters the K_{actin} of chicken myosin Va (*51*), it should be noted that the difference in the K_{actin} values between myosin Va and myosin Vb is due to the difference in the heavy chain but not light chains because the K_{actin} of myosin Vb is significantly higher than that of mammalian myosin Va having calmodulin as light chains but not essential light chain (*41*, *43*). The ATP dependence of the actin-activated ATPase activity of M5BS1 also followed the Michaelis−Menten equation, and a K_{ATP} value of 28.1 ± 5.9 μM was obtained (Figure 4). This value was significantly higher than that of mouse myosin Va (9.6 ± 0.8 μM) (S. Watanabe and M. Ikebe, unpublished observation).

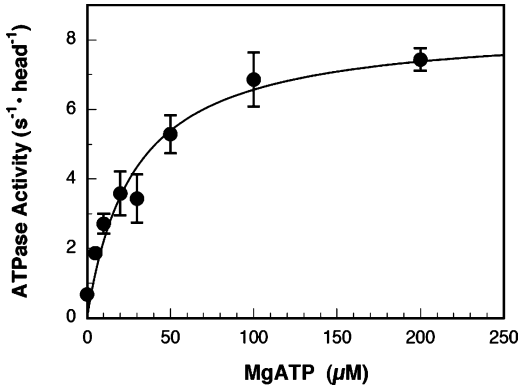

FIGURE 4: ATP concentration dependence of the actin-activated ATPase activity of M5BS1. The assay conditions were the same as those described in the legend of Figure 3, except that a fixed F-actin concentration (30 μM) was used. The solid line is the fit to the Michaelis−Menten equation with a V_{max} of 8.4 ± 0.7 s^{-1} and a K_{ATP} of 28.1 ± 5.9 μM. Error bars represent standard deviations of three independent experiments.

It has been shown that the actin-activated ATPase activity of myosin Va is markedly attenuated with reaction time, and this is due to the inhibition of the activity by ADP produced during the course of the ATPase reaction (*52*). As shown in Figure 5A, the actin-activated ATPase activity of M5BS1 was markedly diminished with time when the reaction was carried out in the absence of the ATP regeneration system, while the inhibition was eliminated in the presence of the ATP regeneration system. The result suggests that the actin-activated ATPase activity of M5BS1 is significantly inhibited by ADP. To further ensure this issue, the activity was measured as a function of ADP concentration (Figure 5B). The ATPase activity was inhibited by ADP, and a K_{ADP} of 3.7 ± 0.4 μM was obtained on the basis of the fitting of the data to the equation $v = V_{max}[ATP]/[K_{ATP}(1 + [ADP]/K_{ADP}) + [ATP]]$. Strong inhibition of the ATPase activity by ADP was found for myosin Va and myosin VI but not myosin II, and it has been thought that this is due to the fact that the rate-limiting step is ADP dissociation for the actin-activated ATPase cycle of myosin Va and myosin VI. Therefore, these results suggest that the predominant intermediate of the acto-M5BS1 ATPase cycle is the ADP-bound form that is a strong actin binding intermediate. To address this notion more directly, we measured the kinetic parameters of M5BS1. Figure 6 shows the rates of binding of mant-ATP to M5BS1 (Figure 6A) and acto-M5BS1 (Figure 6B) as a function of the mant-ATP concentration. For M5BS1 and acto-M5BS1, the time courses of mant fluorescence enhancement followed single-exponential kinetics, and the mant-ATP binding rate increased linearly with mant-ATP concentration. On the basis of Scheme 1, where A and M represent actin and myosin head, respectively, the second-order rate constants for ATP

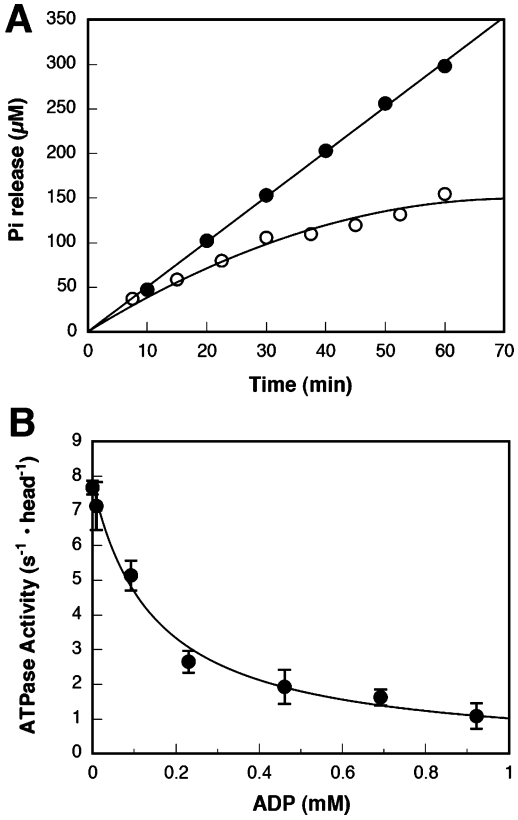

FIGURE 5: Inhibition of the actin-activated ATPase activity of M5BS1 by ADP. (A) Effect of the ATP regeneration system on the time course of ATPase activity. The ATPase activity was measured in the presence (●) and absence (○) of phosphoenolpyruvate and pyruvate kinase. The conditions were the same as those described in the legend of Figure 4, except that 11 nM M5BS1 was used. (B) ADP concentration dependence of the ATPase activity. The conditions were the same as those described in the legend of Figure 4, except that 1 mM MgATP was used. The solid line is the calculated one based on the equation $v = V_{max}[ATP]/[K_{ATP}(1 + [ADP]/K_{ADP}) + [ATP]]$. Error bars are standard deviations of three independent experiments.

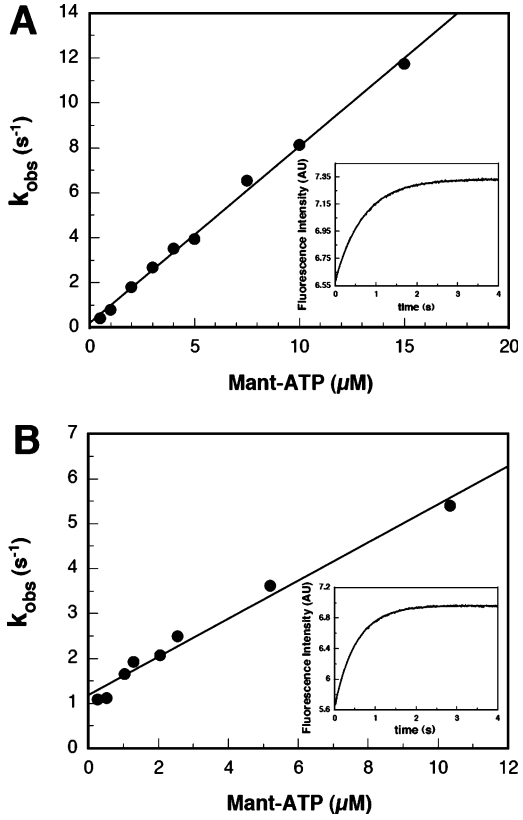

FIGURE 6: Binding of mant-ATP to M5BS1 and actoM5BS1. (A) M5BS1 (0.5 μM) was mixed with various concentrations of 2′-deoxy-mant-ATP. The second-order rate constant for mant-ATP binding (K_1k_2) was 0.78 ± 0.02 μM^{-1} s^{-1}. From the *y*-intercept, a k_{-2} of 0.20 ± 0.12 s^{-1} was obtained. The inset shows the time course of the mant-ATP fluorescence increase after mixing 0.5 μM M5BS1 with 2 μM mant-ATP. The solid line shows the best single-exponential fit with a k_{obs} of 1.8 s^{-1}. (B) Acto-M5BS1 (0.5 μM) was mixed with various concentrations of 2′-deoxy-mant-ATP. The second-order rate constant ($K_1'k_2'$) of 0.42 ± 0.03 μM^{-1} s^{-1} and the k_{-2}' of 1.2 ± 0.1 s^{-1} were obtained. The inset is a time course of the mant-ATP fluorescence change after mixing 0.5 μM acto-M5BS1 with 2.5 μM mant-ATP. The solid line is the best single-exponential fit with a k_{obs} of 2.3 s^{-1}. AU stands for arbitrary units.

binding obtained from the slopes of the linear fits are 0.78 ± 0.02 μM^{-1} s^{-1} for M5BS1 (K_1k_2) and 0.42 ± 0.03 μM^{-1} s^{-1} for acto-M5BS1 ($K_1'k_2'$). From the *y*-intercept, a k_{-2} of 0.20 ± 0.12 s^{-1} for M5BS1 and a k_{-2}' of 1.2 ± 0.1 s^{-1} for acto-M5BS1 were obtained. The result clearly indicated that the ATP-binding step is not the rate-limiting step of the ATPase cycle under physiological conditions. It has been known that actomyosin is quickly dissociated upon the binding of ATP to myosin. As shown in Figure 7A, the rate of acto-M5BS1 dissociation linearly increased with ATP concentration, and a second-order dissociation rate constant of 0.31 ± 0.02 μM^{-1} s^{-1} was obtained from the initial slope of the line. This value is similar to the rate of binding of mant-ATP to acto-M5BS1, suggesting that acto-M5S1 is rapidly dissociated upon ATP binding. On the other hand, the rate of dissociation of acto-M5BS1 by ATP was markedly slowed in the presence of ADP. More importantly, the rate of dissociation quickly plateaued with a maximum value of 12.2 ± 0.5 s^{-1}. The decrease in the rate of ATP-induced acto-M5BS1 dissociation by ADP is due to slow ADP dissociation, and the maximum dissociation rate at high ATP concentrations provides the rate of dissociation of ADP from acto-M5BS1. The rate of dissociation of ADP from acto-M5BS1 was also determined by measuring the fluorescence

Scheme 1

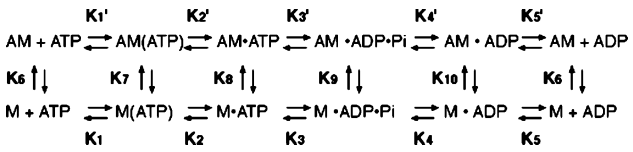

decrease of mant-ADP upon ATP binding (Figure 7B). The transient was best fit to single-exponential kinetics, and the rate of mant-ADP dissociation (k_5') was 11.1 ± 2.1 s^{-1}. The obtained rate constants for dissociation of ADP and mant-ADP from acto-M5BS1 were comparable to the V_{max} of the steady-state ATPase activity, providing evidence that ADP dissociation is the rate-limiting step of the acto-myosin Vb ATPase cycle.

Actin Gliding Activity of Myosin Vb. The results given above suggest that myosin Vb spends a predominant fraction of time as an actin-bound form, i.e., high duty ratio. To further evaluate the high duty ratio of myosin Vb, we measured K_{ATP} of the steady-state ATPase activity and the actin gliding velocity of M5BHMM and compared them. Both the ATPase activity and the actin gliding velocity showed hyperbolic saturation curves and yielded K_{ATP} values

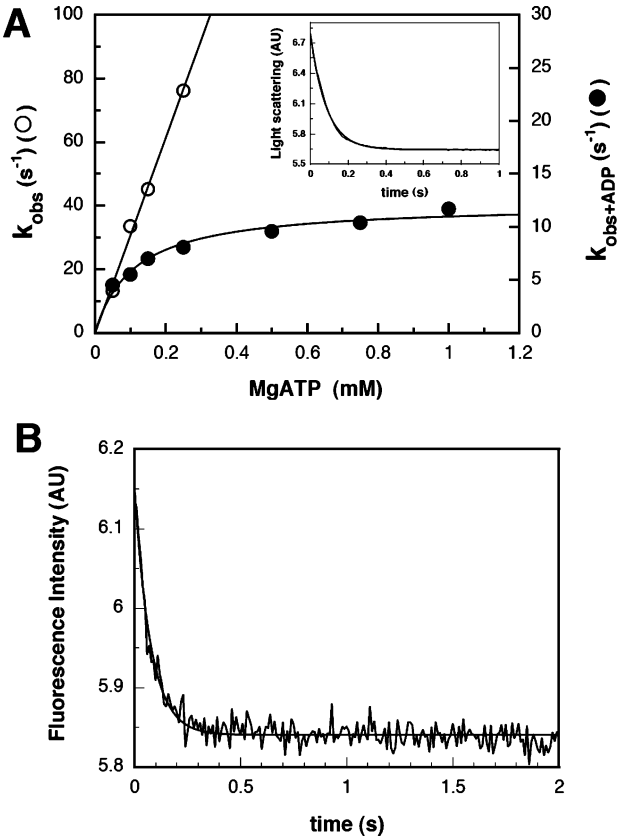

FIGURE 7: Dissociation of ADP from acto-M5BS1. (A) Acto-M5BS1 (0.5 μM) in the presence (●) and absence (○) of 60 μM ADP was mixed with various concentrations of MgATP. From the initial slope of the linear fit in the absence of ADP, the second-order rate constant for ATP binding ($K_1'k_2'$) was 0.31 ± 0.02 μM^{-1} s^{-1}. In the presence of ADP, the observed rates (k_{obs}) were saturated at 12.2 ± 0.5 s^{-1} (k_5'). The inset shows the time course of the change in the light scattering after mixing 0.5 μM acto-M5BS1 and 60 μM ADP with 1 mM MgATP. The solid line shows the best single-exponential fit with a k_{obs} of 11.7 s^{-1}. (B) Dissociation of mant-ADP from acto-M5BS1. MgATP (2 mM) was added to the mixture of 0.5 μM acto-M5BS1 and 20 μM mant-ADP, and the decrease in the fluorescence intensity due to the dissociation of mant-ADP from acto-M5BS1 was monitored. The solid line is the best fit to single-exponential kinetics with a rate of 13.1 s^{-1}. AU stands for arbitrary units.

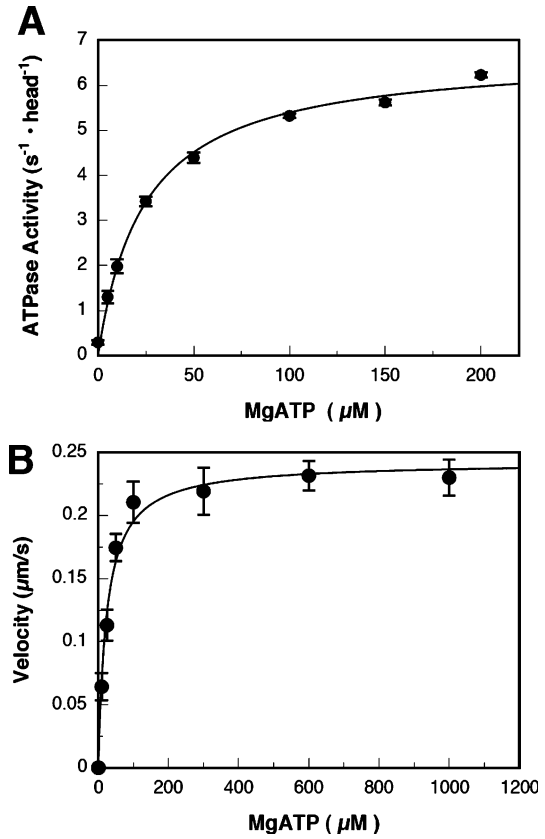

FIGURE 8: ATP dependence of the actin-activated ATPase activity and the actin gliding velocity of M5BHMM. (A) Actin-activated ATPase actitvity. The conditions were the same as those described in the legend of Figure 4. The solid line is the fit to the Michaelis−Menten equation with a V_{max} of 6.7 ± 0.2 s^{-1} (per head) and a K_m of 24.2 ± 2.6 μM. Error bars are standard deviations of three independent experiments. (B) Actin gliding velocity. The fluorescently labeled actin filament movement was observed in 50 mM KCl, 20 mM MOPS-KOH (pH 7.0), 3 mM $MgCl_2$, 1 mM EGTA, 1 mM dithiothreitol, various concentrations of MgATP, 36 μg/mL catalase, 4.5 mg/mL glucose, 216 μg/mL glucose oxidase, and the ATP regeneration system (4 mM phosphoenolpyruvate and 40 units/mL pyruvate kinase) at 25 °C. The solid line is the fit to the Michaelis−Menten equation with a V_{max} of 0.24 ± 0.02 μm/s and a K_m of 24.1 ± 3.0 μM. Error bars are standard deviations for n = 30.

of 24.2 ± 2.6 μM for the ATPase activity (Figure 8A) and 24.1 ± 3.0 μM for the actin gliding velocity (Figure 8B). On the basis of these values, the duty ratio of M5BHMM was estimated to be 1.0. It is therefore anticipated that myosin Vb can be a processive motor. To address this notion, we first measured the actin gliding velocity as a function of surface density of M5BHMM. It is known that nonprocessive myosin such as myosin II markedly decreases its actin gliding activity at a low surface density, while a number of molecules successively bind and move actin filaments to yield a maximum velocity at a high surface density. In contrast, one molecule is sufficient to produce the maximum velocity for a processive motor. Therefore, the velocity does not decrease with a low surface density (*53*). As shown in Figure 9, the actin gliding velocity did not decrease at very low surface densities, suggesting that myosin Vb is a processive myosin. Second, we performed the landing test, which measures the rate at which actin filaments land and move on the surface of a myosin-coated coverslip. The landing rate decreases as the surface density of myosin molecules decreases. If only one myosin molecule is sufficient to support continuous movement, the landing rate exhibits a pseudo-first-order dependence on myosin density (*37*, *54*). When log(landing rate) is plotted against log(motor molecule density), the slope of the obtained straight line provides the order of the landing process. As shown in Figure 10, the slope of the landing process of M5BHMM was best fitted when n = 1. These results indicate that myosin Vb is a processive motor.

On the other hand, the direction of movement of the actin filament by myosin Vb was determined using dual-fluorescence-labeled actin filaments (Figure 11). The minus ends of the filaments led the movement, indicating that myosin Vb is a plus end-directed motor.

DISCUSSION

Myosin constitutes a superfamily (*1*−*7*) and plays a key role in diverse cellular motile processes. Among them, class V myosin is the best studied unconventional myosin and thought to play a role in vesicular trafficking processes in cells (*9*). While mammals have three isoforms of class V

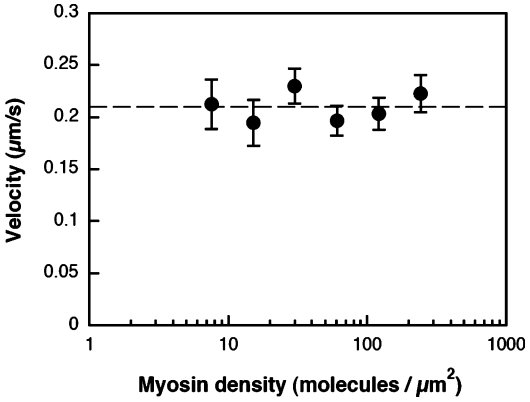

FIGURE 9: Surface density dependence of the actin gliding velocity of M5BHMM. Actin filament velocity was observed in buffer containing 25 mM KCl, 25 mM imidazole (pH 7.5), 5 mM $MgCl_2$, 1 mM EGTA, 1 mM dithiothreitol, 36 μg/mL catalase, 4.5 mg/mL glucose, 216 μg/mL glucose oxidase, 0.5% methylcellulose, and 4 mM MgATP at 25 °C. The amount of protein bound to the flow cell (approximately 50%) was estimated by subtracting the flow-through from the initial concentration determined by a densitometric scan of SDS−PAGE. Error bars represent standard deviations for $n = 20$.

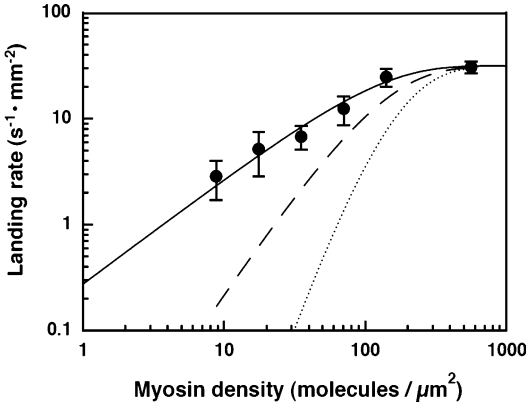

FIGURE 10: Landing rate as a function of surface motor density of M5BHMM. The solid line, dashed line, and dotted line represent the theoretical curves of $n = 1$, 2, and 4, respectively. The landing rate was determined as described in Experimental Procedures. The bars represent standard errors calculated according to the method of Hancock and Howard (*37*) for $n = 10-40$.

myosin, the motor characteristic of myosin V has been studied well for myosin Va, yet nothing has been studied for the other two myosin V isoforms (Vb and Vc). This study clarifies the motor characteristic of myosin Vb for the first time.

To prepare human myosin Vb, we decided to express recombinant myosin Vb rather than to purify it from tissues because it is known that various types of myosins are present in the same tissue and it would be difficult to completely eliminate the contamination of other myosins. Furthermore, the tissue distributions of myosin V isoforms overlap each other (*11*), and one cannot eliminate the contamination of different isoforms.

We produced M5BS1 and M5BHMM constructs. The former contains the entire motor domain and the neck domain where six light chains are bound. This construct was used to study the enzymatic properties of human myosin Vb because this construct is a one-headed form (Figure 2B), thus

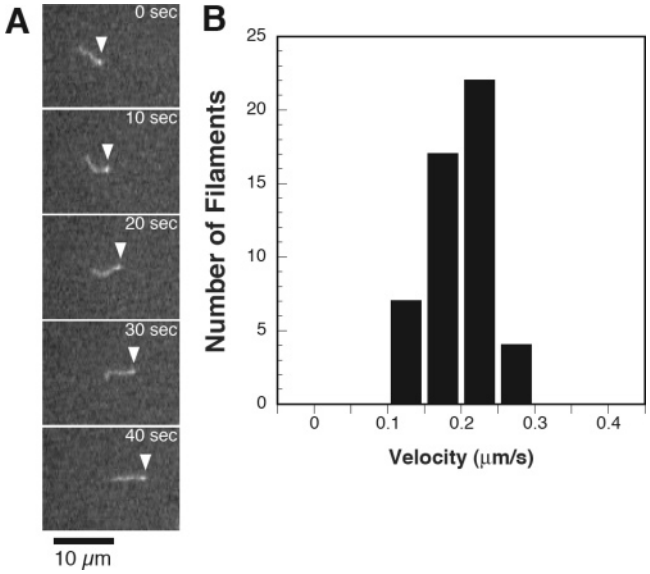

FIGURE 11: Direction of the movement of M5BHMM. (A) Movement of the dual-labeled F-actin filaments was observed. The bright tips of the actin filaments represent the minus end of the filaments. The white arrowheads indicate the leading part of the dual-labeled actin filaments. The minus ends of the filaments lead the movement, indicating that M5BHMM moves toward the barbed end of actin. Times are indicated at the right. (B) Histogram of the velocities of dual-labeled F-actin filaments. Movement toward the barbed end of F-actin is defined as positive values.

preventing the complexity arising from the possible interhead interaction.

The latter contains the coiled-coil domain connected to the neck domain, and as expected, this construct displayed a two-headed structure (Figure 2B). This construct was used for the actin gliding assays because the two-headed construct is suitable for representing the authentic motility properties, including processivity. Furthermore, it has been shown for other myosins that HMM shows better actin gliding activity than S1, presumably due to the undesired binding of the S1 to the glass surface at the head domain (*41*, *55*). On the basis of the amino acid sequence, there are six IQ motifs, the light chain binding motifs, in the neck domain of human myosin Vb. The length of the neck of M5BHMM observed with the electron micrograph was the same as that of myosin Va, suggesting that myosin Vb also contains six bound light chains. It is also consistent with the number of bound calmodulins determined by the densitometry analysis of SDS−PAGE.

Table 1 shows the comparison of the kinetic and motility parameters for human myosin Vb, mammalian Va, and *Drosophila* myosin V. Overall, human myosin Vb is highly homologous to myosin Va, with 62% of its amino acids identical to those of human myosin Va in the entire length and 74% identical in the motor head domain. This high degree of homology of the myosin Vb sequence to the myosin Va sequence is consistent with the similarity of the mechanoenzymatic properties of myosin Vb and myosin Va, i.e., the slow ADP dissociation rate. However, there are the regions in the motor domain of myosin Vb whose sequences are quite different from that of myosin Va. Among them, of interest is the loop 2 region that has been suggested to influence the actin binding property of myosin (*43*−*47*) since the K_{actin} of myosin Vb is significantly higher than that of

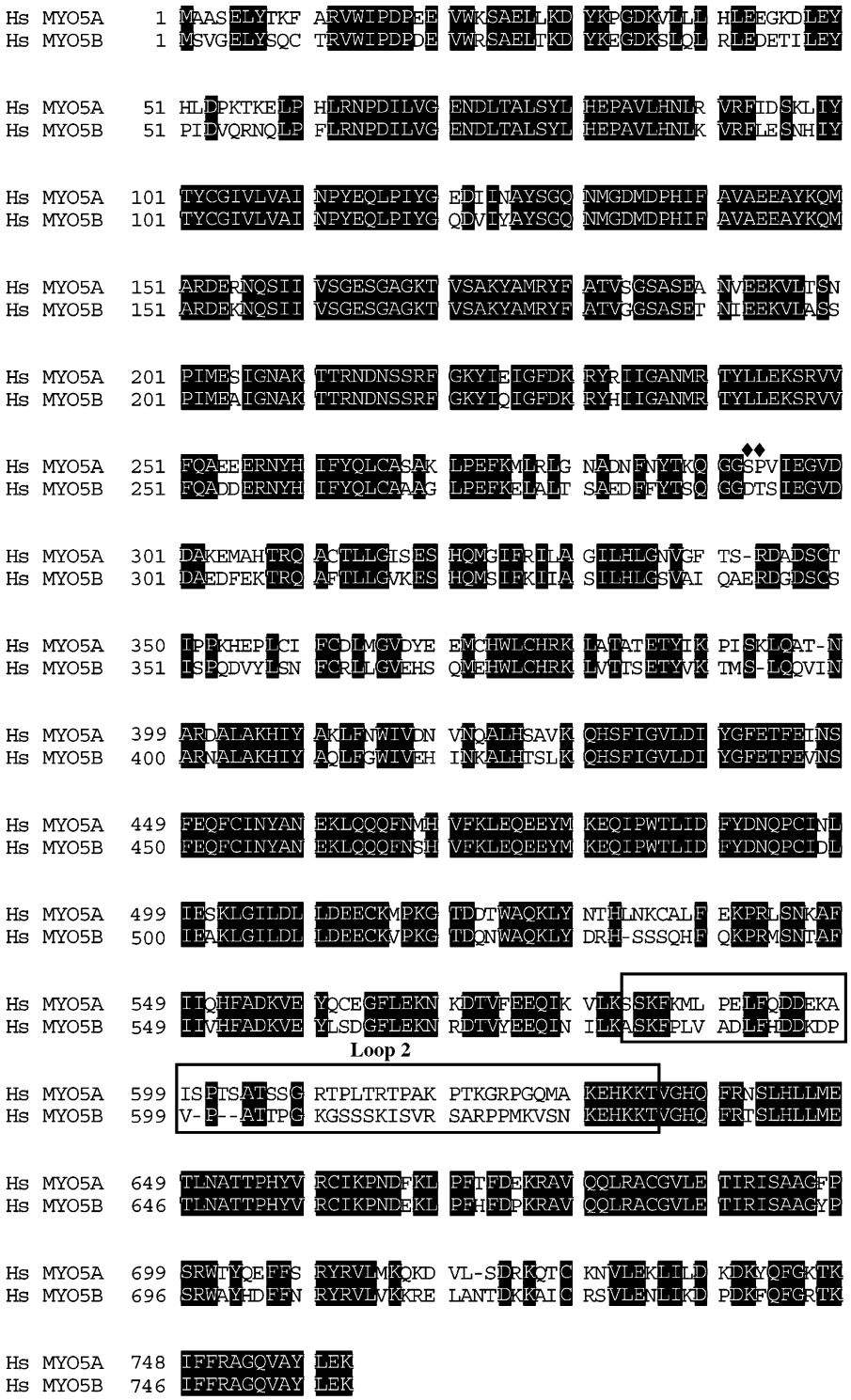

FIGURE 12: Alignment of amino acid sequences in the motor domains between human myosin Va and Vb. Highlighted letters denote the identical residues in myosin Va and Vb. Human myosin Va and Vb are 74% identical in the motor domain. However, the sequence of loop 2 in myosin Vb is quite different from that of myosin Va. Between the residues indicated by ◆, myosin VI has a unique insertion that alters the rate of ATP binding (*57*). Hs stands for *Homo sapiens*.

myosin Va. Figure 12 shows the amino acid sequence comparison between human myosin Va and myosin Vb in the motor domain. The loop 2 sequence of myosin Vb is unique and quite different from that of myosin Va. Recently, it was shown that the mutation of loop 2 of myosin Va significantly changed the K_{actin} value but not the V_{max} of the actin-activated ATPase activity of myosin Va (*56*). It is plausible that the difference in loop 2 is responsible for the difference in the K_{actin} between the two isoforms.

We also found that the K_{ATP} of myosin Vb is significantly higher than that of myosin Va. This is primarily due to the difference in the ATP binding rate that is ~2.5 times slower than that of myosin Va and the presence of the reverse reaction of the ATP-binding step. Recently, it was reported that the truncation of the insertion unique to myosin VI in the upper 50 kDa domain significantly increased the rate of

ATP binding (*57*). The insertion is located between positions 293 and 294 in the myosin Vb sequence (indicated by ◆ in Figure 12), in which the amino acid residues are different between the two isoforms. It is plausible that this region is responsible for the reduced affinity of myosin Vb for ATP.

The V_{max} of the actin-activated ATPase activity of myosin Vb was approximately two-thirds of that of myosin Va, which is significantly lower than that of myosin Va (*12*, *42*). The slower cycling rate is also consistent with the actin gliding velocity; myosin Vb exhibited approximately two-thirds of the velocity of myosin Va (*43*, *58*).

The actin-activated ATPase activity of the single-headed M5BS1 construct was significantly reduced with reaction time when the reaction was carried out without the ATP regeneration system, suggesting that ADP significantly inhibits the ATPase activity. This was confirmed by measuring the effect of ADP on the ATPase activity that resulted in the strong inhibition of the activity. These results suggest that the ADP dissociation step limits the rate of the overall ATPase cycle. This is consistent with the result that the rate of dissociation of ADP from acto-M5BS1 is comparable to the actin-activated steady-state ATPase rate. An approximate duty ratio can be estimated by dividing the rate of ADP dissociation by the steady-state V_{max}. The duty ratio of M5BS1 is calculated to be 0.79, indicating that M5BS1 has a high duty ratio and spends a majority of the time during the cycle with the strongly actin bound state. In this study, it was demonstrated that myosin Vb is a double-headed structure (Figure 2B). A high duty ratio of >0.5 of single-headed M5BS1 suggests that double-headed myosin Vb is a processive motor that undergoes multiple steps along actin filaments before detaching. This was also supported by the comparison of K_{ATP} values for the actin-activated ATPase activity and the actin gliding velocity of M5BHMM that resulted in a K_{ATP}(ATPase)/K_{ATP}(motility) of nearly 1.0.

To further clarify whether myosin Vb is a processive motor, we examined the in vitro actin gliding activity of myosin Vb. The actin gliding velocity did not attenuate at a low surface density of myosin Vb. Furthermore, the landing test indicated that the plot of the landing rate versus myosin Vb surface density was best fitted with an n of 1, suggesting that a single myosin Vb molecule is sufficient to drive the movement of an actin filament. These results clearly indicate that myosin Vb is a processive myosin similar to myosin Va. The average size of displacement, d, over which the cross bridge remains attached to actin during the power stroke, can be estimated by the dependence of the motility at a submaximal MgATP concentration (k_{max}/K_{app}) based upon the following equation (*59*).

$$d = (k_{max}/K_{app})/K_1'k_2' = (0.22\ \mu\text{m s}^{-1}/2.4 \times 10^{-5}\ \text{M})/(3.1 \times 10^5\ \text{M}^{-1}\ \text{s}^{-1}) = 30\ \text{nm}$$

This value is similar to the step size (36 nm) of myosin Va (*13*, *15*). Therefore, it is reasonable to assume that myosin Vb moves on actin filaments with large steps in a manner similar to that of myosin Va.

This study clearly demonstrates that myosin Vb is a processive motor that moves on actin filaments for a long distance without dissociating from actin. Furthermore, we have also demonstrated that myosin Vb is a plus end-directed motor. Recent studies have revealed that myosin Vb associates with members of the Rab11 family and is involved in the receptor recycling system in cells and suggested that myosin Vb functions as a transporter of cargo from the pericentrosomal region to the plasma membrane. These findings agree with these cell biological findings and provide the molecular basis for the function of myosin Vb as a cargo carrier motor protein in cells.

REFERENCES

1. Cheney, R. E., Riley, M. A., and Mooseker, M. S. (1993) Phylogenetic analysis of the myosin superfamily, *Cell Motil. Cytoskeleton 24*, 215−223.
2. Goodson, H. V., and Spudich, J. A. (1993) Molecular evolution of the myosin family: Relationships derived from comparisons of amino acid sequences, *Proc. Natl. Acad. Sci. U.S.A. 90*, 659−663.
3. Mooseker, M. S., and Cheney, R. E. (1995) Unconventional myosins, *Annu. Rev. Cell Dev. Biol. 11*, 633−675.
4. Cope, M. J., Whisstock, J., Rayment, I., and Kendrick-Jones, J. (1996) Conservation within the myosin motor domain: Implications for structure and function, *Structure 4*, 969−987.
5. Baker, J. P., and Titus, M. A. (1997) A family of unconventional myosins from the nematode *Caenorhabditis elegans*, *J. Mol. Biol. 272*, 523−535.
6. Hodge, T., and Cope, M. J. (2000) A myosin family tree, *J. Cell Sci. 113* (Part 19), 3353−3354.
7. Berg, J. S., Powell, B. C., and Cheney, R. E. (2001) A millennial myosin census, *Mol. Biol. Cell 12*, 780−794.
8. Mercer, J. A., Seperack, P. K., Strobel, M. C., Copeland, N. G., and Jenkins, N. A. (1991) Novel myosin heavy chain encoded by murine dilute coat colour locus, *Nature 349*, 709−713.
9. Reck-Peterson, S. L., Provance, D. W., Jr., Mooseker, M. S., and Mercer, J. A. (2000) Class V myosins, *Biochim. Biophys. Acta 1496*, 36−51.
10. Zhao, L. P., Koslovsky, J. S., Reinhard, J., Bahler, M., Witt, A. E., Provance, D. W., Jr., and Mercer, J. A. (1996) Cloning and characterization of myr 6, an unconventional myosin of the dilute/myosin-V family, *Proc. Natl. Acad. Sci. U.S.A. 93*, 10826−10831.
11. Rodriguez, O. C., and Cheney, R. E. (2002) Human myosin-Vc is a novel class V myosin expressed in epithelial cells, *J. Cell Sci. 115*, 991−1004.
12. De La Cruz, E. M., Wells, A. L., Rosenfeld, S. S., Ostap, E. M., and Sweeney, H. L. (1999) The kinetic mechanism of myosin V, *Proc. Natl. Acad. Sci. U.S.A. 96*, 13726−13731.
13. Mehta, A. D., Rock, R. S., Rief, M., Spudich, J. A., Mooseker, M. S., and Cheney, R. E. (1999) Myosin-V is a processive actin-based motor, *Nature 400*, 590−593.
14. Sakamoto, T., Amitani, I., Yokota, E., and Ando, T. (2000) Direct observation of processive movement by individual myosin V molecules, *Biochem. Biophys. Res. Commun. 272*, 586−590.
15. Tanaka, H., Homma, K., Iwane, A. H., Katayama, E., Ikebe, R., Saito, J., Yanagida, T., and Ikebe, M. (2002) The motor domain determines the large step of myosin-V, *Nature 415*, 192−195.
16. Veigel, C., Wang, F., Bartoo, M. L., Sellers, J. R., and Molloy, J. E. (2002) The gated gait of the processive molecular motor, myosin V, *Nat. Cell Biol. 4*, 59−65.
17. Walker, M. L., Burgess, S. A., Sellers, J. R., Wang, F., Hammer, J. A., III, Trinick, J., and Knight, P. J. (2000) Two-headed binding of a processive myosin to F-actin, *Nature 405*, 804−807.
18. Rief, M., Rock, R. S., Mehta, A. D., Mooseker, M. S., Cheney, R. E., and Spudich, J. A. (2000) Myosin-V stepping kinetics: A molecular model for processivity, *Proc. Natl. Acad. Sci. U.S.A. 97*, 9482−9486.
19. De La Cruz, E. M., Ostap, E. M., and Sweeney, H. L. (2001) Kinetic mechanism and regulation of myosin VI, *J. Biol. Chem. 276*, 32373−32381.
20. Watanabe, T. M., Tanaka, H., Iwane, A. H., Maki-Yonekura, S., Homma, K., Inoue, A., Ikebe, R., Yanagida, T., and Ikebe, M. (2004) A one-headed class V myosin molecule develops multiple large (∼32-nm) steps successively, *Proc. Natl. Acad. Sci. U.S.A. 101*, 9630−9635.
21. Nascimento, A. A., Amaral, R. G., Bizario, J. C., Larson, R. E., and Espreafico, E. M. (1997) Subcellular localization of myosin-V in the B16 melanoma cells, a wild-type cell line for the dilute gene, *Mol. Biol. Cell 8*, 1971−1988.

22. Wu, X., Bowers, B., Wei, Q., Kocher, B., and Hammer, J. A., III (1997) Myosin V associates with melanosomes in mouse melanocytes: Evidence that myosin V is an organelle motor, *J. Cell Sci. 110* (Patt 7), 847−859.
23. Takagishi, Y., Oda, S., Hayasaka, S., Dekker-Ohno, K., Shikata, T., Inouye, M., and Yamamura, H. (1996) The dilute-lethal (dl) gene attacks a Ca^{2+} store in the dendritic spine of Purkinje cells in mice, *Neurosci. Lett. 215*, 169−172.
24. Lapierre, L. A., Kumar, R., Hales, C. M., Navarre, J., Bhartur, S. G., Burnette, J. O., Provance, D. W., Jr., Mercer, J. A., Bahler, M., and Goldenring, J. R. (2001) Myosin vb is associated with plasma membrane recycling systems, *Mol. Biol. Cell 12*, 1843−1857.
25. Fan, G. H., Lapierre, L. A., Goldenring, J. R., Sai, J., and Richmond, A. (2004) Rab11-family interacting protein 2 and myosin Vb are required for CXCR2 recycling and receptor-mediated chemotaxis, *Mol. Biol. Cell 15*, 2456−2469.
26. Volpicelli, L. A., Lah, J. J., Fang, G., Goldenring, J. R., and Levey, A. I. (2002) Rab11a and myosin Vb regulate recycling of the M4 muscarinic acetylcholine receptor, *J. Neurosci. 22*, 9776−9784.
27. Provance, D. W., Jr., Gourley, C. R., Silan, C. M., Cameron, L. C., Shokat, K. M., Goldenring, J. R., Shah, K., Gillespie, P. G., and Mercer, J. A. (2004) Chemical-genetic inhibition of a sensitized mutant myosin Vb demonstrates a role in peripheral-pericentriolar membrane traffic, *Proc. Natl. Acad. Sci. U.S.A. 101*, 1868−1873.
28. Toth, J., Kovacs, M., Wang, F., Nyitray, L., and Sellers, J. R. (2005) Myosin V from *Drosophila* reveals diversity of motor mechanisms within the myosin V family, *J. Biol. Chem*. (in press).
29. Spudich, J. A., and Watt, S. (1971) The regulation of rabbit skeletal muscle contraction. I. Biochemical studies of the interaction of the tropomyosin-troponin complex with actin and the proteolytic fragments of myosin, *J. Biol. Chem. 246*, 4866−4871.
30. Laemmli, U. K. (1970) Cleavage of structural proteins during the assembly of the head of bacteriophage T4, *Nature 227*, 680−685.
31. Mabuchi, K. (1990) Melting of myosin and tropomyosin: Electron microscopic observations, *J. Struct. Biol. 103*, 249−256.
32. Mabuchi, K. (1991) Heavy-meromyosin-decorated actin filaments: A simple method to preserve actin filaments for rotary shadowing, *J. Struct. Biol. 107*, 22−28.
33. Reynard, A. M., Hass, L. F., Jacobsen, D. D., and Boyer, P. D. (1961) The correlation of reaction kinetics and substrate binding with the mechanism of pyruvate kinase, *J. Biol. Chem. 236*, 2277−2283.
34. Ikebe, M., and Hartshorne, D. J. (1985) Effects of Ca^{2+} on the conformation and enzymatic activity of smooth muscle myosin, *J. Biol. Chem. 260*, 13146−13153.
35. Sata, M., Matsuura, M., and Ikebe, M. (1996) Characterization of the motor and enzymatic properties of smooth muscle long S1 and short HMM: Role of the two-headed structure on the activity and regulation of the myosin motor, *Biochemistry 35*, 11113−11118.
36. Homma, K., Yoshimura, M., Saito, J., Ikebe, R., and Ikebe, M. (2001) The core of the motor domain determines the direction of myosin movement, *Nature 412*, 831−834.
37. Hancock, W. O., and Howard, J. (1998) Processivity of the motor protein kinesin requires two heads, *J. Cell Biol. 140*, 1395−1405.
38. Rock, R. S., Rice, S. E., Wells, A. L., Purcell, T. J., Spudich, J. A., and Sweeney, H. L. (2001) Myosin VI is a processive motor with a large step size, *Proc. Natl. Acad. Sci. U.S.A. 98*, 13655−13659.
39. White, H. D., and Taylor, E. W. (1976) Energetics and mechanism of actomyosin adenosine triphosphatase, *Biochemistry 15*, 5818−5826.
40. Espindola, F. S., Suter, D. M., Partata, L. B., Cao, T., Wolenski, J. S., Cheney, R. E., King, S. M., and Mooseker, M. S. (2000) The light chain composition of chicken brain myosin-Va: Calmodulin, myosin-II essential light chains, and 8-kDa dynein light chain/PIN, *Cell Motil. Cytoskeleton 47*, 269−281.
41. Wang, F., Chen, L., Arcucci, O., Harvey, E. V., Bowers, B., Xu, Y., Hammer, J. A., III, and Sellers, J. R. (2000) Effect of ADP and ionic strength on the kinetic and motile properties of recombinant mouse myosin V, *J. Biol. Chem. 275*, 4329−4335.
42. Li, X. D., Mabuchi, K., Ikebe, R., and Ikebe, M. (2004) Ca^{2+}-induced activation of ATPase activity of myosin Va is accompanied with a large conformational change, *Biochem. Biophys. Res. Commun. 315*, 538−545.
43. Homma, K., Saito, J., Ikebe, R., and Ikebe, M. (2000) Ca^{2+}-dependent regulation of the motor activity of myosin V, *J. Biol. Chem. 275*, 34766−34771.
44. Margossian, S. S., and Lowey, S. (1973) Substructure of the myosin molecule. IV. Interactions of myosin and its subfragments with adenosine triphosphate and F-actin, *J. Mol. Biol. 74*, 313−330.
45. Wagner, P. D., Slater, C. S., Pope, B., and Weeds, A. G. (1979) Studies on the actin activation of myosin subfragment-1 isoezymes and the role of myosin light chains, *Eur. J. Biochem. 99*, 385−394.
46. Ikebe, M., Koretz, J., and Hartshorne, D. J. (1988) Effects of phosphorylation of light chain residues threonine 18 and serine 19 on the properties and conformation of smooth muscle myosin, *J. Biol. Chem. 263*, 6432−6437.
47. Ikebe, M., and Hartshorne, D. J. (1985) Proteolysis of smooth muscle myosin by *Staphylococcus aureus* protease: Preparation of heavy meromyosin and subfragment 1 with intact 20000-dalton light chains, *Biochemistry 24*, 2380−2387.
48. Truong, T., Medley, Q. G., and Cote, G. P. (1992) Actin-activated Mg-ATPase activity of *Dictyostelium* myosin II. Effects of filament formation and heavy chain phosphorylation, *J. Biol. Chem. 267*, 9767−9772.
49. Kovacs, M., Wang, F., Hu, A., Zhang, Y., and Sellers, J. R. (2003) Functional divergence of human cytoplasmic myosin II: Kinetic characterization of the non-muscle IIA isoform, *J. Biol. Chem. 278*, 38132−38140.
50. Wang, F., Kovacs, M., Hu, A., Limouze, J., Harvey, E. V., and Sellers, J. R. (2003) Kinetic mechanism of non-muscle myosin IIB: Functional adaptations for tension generation and maintenance, *J. Biol. Chem. 278*, 27439−27448.
51. De La Cruz, E. M., Wells, A. L., Sweeney, H. L., and Ostap, E. M. (2000) Actin and light chain isoform dependence of myosin V kinetics, *Biochemistry 39*, 14196−14202.
52. De La Cruz, E. M., Sweeney, H. L., and Ostap, E. M. (2000) ADP inhibition of myosin V ATPase activity, *Biophys. J. 79*, 1524−1529.
53. Rock, R. S., Rief, M., Mehta, A. D., and Spudich, J. A. (2000) In vitro assays of processive myosin motors, *Methods 22*, 373−381.
54. Howard, J., Hudspeth, A. J., and Vale, R. D. (1989) Movement of microtubules by single kinesin molecules, *Nature 342*, 154−158.
55. Morris, C. A., Wells, A. L., Yang, Z., Chen, L. Q., Baldacchino, C. V., and Sweeney, H. L. (2003) Calcium functionally uncouples the heads of myosin VI, *J. Biol. Chem. 278*, 23324−23330.
56. Yengo, C. M., and Sweeney, H. L. (2004) Functional role of loop 2 in myosin V, *Biochemistry 43*, 2605−2612.
57. Yengo, C. M., and Sweeney, H. L. (2004) Myosin VI mutant alters ATP-binding and ADP-release, *Biophys. J. 86*, 30a.
58. Cheney, R. E., O'Shea, M. K., Heuser, J. E., Coelho, M. V., Wolenski, J. S., Espreafico, E. M., Forscher, P., Larson, R. E., and Mooseker, M. S. (1993) Brain myosin-V is a two-headed unconventional myosin with motor activity, *Cell 75*, 13−23.
59. White, H. D., Belknap, B., and Jiang, W. (1993) Kinetics of binding and hydrolysis of a series of nucleoside triphosphates by actomyosin-S1. Relationship between solution rate constants and properties of muscle fibers, *J. Biol. Chem. 268*, 10039−10045.

BI051682B